The Astrophysical Journal Letters, 898:L7 (6pp), 2020 July 20 https://doi.org/10.3847/2041-8213/aba12b

Predicted Masses of Galactic Cepheids in the Gaia Data Release 2

Marcella Marconi[1], Giulia De Somma[1,2,3], Vincenzo Ripepi[1], Roberto Molinaro[1], Ilaria Musella[1], Silvio Leccia[1], and Maria Ida Moretti[1]

[1] INAF—Osservatorio Astronomico di Capodimonte, Via Moiariello 16, I-80131 Napoli, Italy; giulia.desomma@inaf.it, gdesomma@na.infn.it
[2] Dipartimento di Fisica "E. Pancini," Universitá di Napoli "Federico II," Compl. Univ. di Monte S. Angelo, Edificio G, Via Cinthia, I-80126 Napoli, Italy
[3] INFN—Sez. di Napoli Compl. Univ. di Monte S. Angelo, Edificio G, Via Cinthia, I-80126 Napoli, Italy
Received 2020 June 9; revised 2020 June 23; accepted 2020 June 29; published 2020 July 17

Abstract

On the basis of recently computed nonlinear convective pulsation models of Galactic Cepheids, spanning wide ranges of input stellar parameters, we derive theoretical mass-dependent Period–Wesenheit relations in the Gaia bands, namely, G, G_{BP}, and G_{BR}, that are found to be almost independent of the assumed efficiency of superadiabatic convection. The application to a selected subsample of the Gaia Data Release 2 Galactic Cepheids database allows us to derive mass-dependent estimates of their individual distances. By imposing their match with the astrometric values inferred from Gaia, we are able to evaluate the individual mass of each pulsator. The inferred mass distribution is peaked around $5.6M_{\odot}$ and $5.4M_{\odot}$ for the F and FO pulsators, respectively. If the estimated Gaia parallax offset $\langle\Delta\varpi\rangle = 0.046$ mas is applied to Gaia parallaxes before imposing their coincidence with the theoretical ones, the inferred mass distribution is found to shift toward lower masses, namely, $\sim 5.2M_{\odot}$ and $5.1M_{\odot}$ for the F and FO pulsators, respectively. The comparison with independent evaluations of the stellar masses, for a subset of binary Cepheids in our sample, seems to support the predictive capability of the current theoretical scenario. By forcing the coincidence of our mass determinations with these literature values we derive an independent estimate of the mean offset to be applied to Gaia DR2 parallaxes, $\langle\Delta\varpi\rangle = 0.053 \pm 0.029$ mas, slightly higher but in agreement within the errors with the Riess et al. value.

Unified Astronomy Thesaurus concepts: Cepheid variable stars (218); Cepheid distance (217); Distance indicators (394); Stellar pulsations (1625); Stellar oscillations (1617); Stellar evolution (1599)

Supporting material: machine-readable table

1. Introduction

Classical Cepheids (CC) are massive and intermediate-mass ($\sim$3–13 $M_{\odot}$) stars crossing the pulsation instability strip while evolving along the central helium burning phase (see, e.g., Chiosi et al. 1993; Bono et al. 2000; Anderson et al. 2016, and references therein). Thanks to their characteristic period–luminosity (PL) and period–luminosity–color (PLC) relations, they are considered the most important primary distance indicators within the Local Group, currently adopted to calibrate secondary distance indicators and, in turn, to evaluate the Hubble constant (see, e.g., Freedman et al. 2001; Riess et al. 2011, 2018, 2019; Ripepi et al. 2019, and references therein). From the physical point of view, the occurrence of PL and PLC relations relies on the existence of the period-mean density relation coupled with the Stefan-Boltzmann law and the mass–luminosity (ML) relation predicted by stellar evolution models for central helium burning massive and intermediate-mass stars (see, e.g., Bono et al. 1999a, 2000; Chiosi et al. 1993). This implies that any phenomenon affecting the CC ML relation also affects the coefficients of the resulting PL and PLC relations and, in turn, the associated distance scale. Theoretical evaluations of Cepheid masses based on stellar evolution models depend on the assumed ML relation (see, e.g., Cassisi & Salaris 2011) that is affected by chemical composition and physical ingredients such as opacity (see, e.g., the new study by suggesting that opacity might be underestimated; Bailey et al. 2015), equation of state, and nuclear cross sections as well as by macroscopic phenomena, such as core overshooting, mass loss, and rotation. On the other hand, theoretical attempts to derive Cepheid masses from stellar pulsation (see, e.g., Bono et al. 2001; Caputo et al. 2005; Keller & Wood 2006; Marconi et al. 2013a, 2013b, 2017; Ragosta et al. 2019, and references therein) do provide systematically lower masses than evolutionary estimates unless the latter adopt a moderate efficiency of core overshooting in the previous hydrogen burning phase, and/or mass loss and/or rotation. All these effects make the ML relation brighter than for canonical no mass loss, no rotation, and no overshooting models. We notice that such a moderately brighter ML relation also allows us to match dynamical stellar mass derivations for Cepheids in eclipsing binary systems (see, e.g., Pietrzyński et al. 2010, 2011; Neilson & Langer 2012; Prada Moroni et al. 2012; Marconi et al. 2013a). In a recent theoretical investigation of Galactic Classical Cepheid (GCC) properties (see De Somma et al. 2020, hereafter DS2020) based on nonlinear convective models (see Bono et al. 1999b; Marconi et al. 2005, and references therein, for the physical and numerical assumptions), we predicted the light curves and the mean magnitudes and colors in the Gaia filters for classical Cepheid pulsators at solar chemical composition. The inferred period–Wesenheit (PW) relations were applied to a sample of Gaia Data Release 2 (hereinafter DR2) to constrain their individual distances and parallaxes (for details see, e.g., De Somma et al. 2020). The results of this procedure and the comparison of the obtained values with Gaia DR2 observed parallaxes (see Clementini et al. 2019; Ripepi et al. 2019) were found to depend on the assumed ML relation. In this Letter we reverse the perspective and rely on Gaia DR2 (Gaia Collaboration et al. 2018, 2016) parallaxes to constrain GCC individual masses through inversion of predicted mass-dependent PW relations, thus testing a tool that will be fully efficient when the

Table 1
The Coefficients of the PWM Relation ($W = a + b\log P + c\log M/M_{\odot}$) Predicted for the F- and FO-mode GCCs, Varying the Mixing Length Parameter

$\alpha_{\rm ml}$	a	b	c	σ_a	σ_b	σ_c	σ
F							
1.5	−1.654	−2.419	−2.423	0.036	0.021	0.067	0.064
1.7	−1.686	−2.496	−2.285	0.040	0.026	0.082	0.058
FO							
1.5	−2.162	−3.068	−1.819	0.023	0.020	0.044	0.013
1.7	−2.205	−3.093	−1.765	0.032	0.027	0.062	0.008

Note. The last column represents the rms deviation (σ) coefficient.

final Gaia data release will be available. The organization of the Letter is as follows. In Section 2, we derive the mass-dependent PW relations from the nonlinear convective models computed by De Somma et al. 2020. In Section 3, we present the selected Cepheid sample and the procedure to derive individual masses. In Section 4, we compare the obtained individual masses with independent results for Cepheids in binary systems in the literature. Finally, Section 5 includes a discussion of results with some future developments.

2. The Mass-dependent Period–Wesenheit Relations

The predicted intensity weighted mean magnitudes and colors in the Gaia filters, $\langle G\rangle$, $\langle G_{\rm BP}\rangle$, and $\langle G_{\rm BR}\rangle$, provided by De Somma et al. (2020) for the extensive grid of pulsation models computed at solar chemical composition, depend on the assumed ML relation. In particular, for each stellar mass, three luminosity levels are considered in that paper, corresponding to a canonical value (case A, neglecting core-overshooting, mass-loss, and rotation effects) based on evolutionary predictions by Bono et al. (2000) and two additional noncanonical luminosity levels obtained by increasing the canonical luminosity by 0.2 dex (case B) and 0.4 dex (case C). Considering this whole model set, for each combination of mass, luminosity, and effective temperature we can provide the corresponding predicted period and Wesenheit function[4] and, in turn, derive the mass-dependent period–Wesenheit (hereinafter PWM) relations for the fundamental (F) and first overtone (FO) models, on the same period range as for the observed GCC. The coefficients of the predicted relations for both F and FO models are reported in Table 1 for the two assumptions on the efficiency of superadiabatic convection, namely, $\alpha = 1.5$[5] and $\alpha = 1.7$. We notice that a variation in the α parameter does not significantly affect the coefficients of the PWM relations, in spite of significant effects on the amplitude and morphology of light curves (for details see Bhardwaj et al. 2017; De Somma et al. 2020). For this reason, in the following we only consider model predictions for $\alpha = 1.5$. Among other parameters involved in the time-dependent convective treatment (see Bono & Stellingwerf 1994 for details), the eddy viscosity coefficient $\nu_{\rm eddy}$ is set independently of the mixing length, whereas the overshooting length scale is related to α. A variation of $\nu_{\rm eddy}$ is expected to produce similar effects on the light-curve amplitudes, morphology, and the instability strip width as the α changes, but not to significantly affect the derivation of the PWM relations. Moreover, we notice that, for Cepheid samples at the same distance, such relations allow us to constrain the stellar mass distribution, whereas in the case of available individual distances, as for the Gaia database, the absolute individual mass values are directly determined. In Figure 1 we plot the derived F (green symbols) and FO (red symbols) model distribution in the $W - c\log M$ versus $\log P$ plane, overimposed on the projection of the inferred PWM relations. These relations will be used in the following section to infer individual mass estimates for a sample of GCCs with Gaia DR2 distances.

3. Application to Gaia DR2 Galactic Cepheids

In this section, we present a first test of the predictive capability of the derived PWM relations for the F and FO pulsators through their application to a subset of Gaia DR2 GCCs (see DS2020; Ripepi et al. 2019).

3.1. The Selected Sample

The adopted sample of Gaia DR2 GCC is the one compiled by Ripepi et al. (2019) and used in DS2020 to derive theoretical distances. In the present work, in order to convert the observed Gaia parallaxes into distance moduli $\mu_{\rm Gaia}$, then used to correct apparent Wesenheit magnitudes, we selected only Cepheids in the Ripepi et al. (2019) sample with a relative error on Gaia DR2 parallax lower than 10% and positive mean parallax values. Table 2, from columns 1 to 8, reports the Gaia source identification, the pulsation mode, the pulsation period, the mean apparent magnitudes in the Gaia filters, the measured parallax, and the associated uncertainty of the selected GCC. In the following we use these observed properties to constrain the individual stellar masses, through application of theoretical PWM relations.

3.2. Derivation of Individual Cepheid Masses

From the equation

$$W_{\rm oss} - \mu_{\rm Gaia} = W_{\rm teo} = a + b\log P + c\log M/M_{\odot},$$

where W_{oss} is defined as

$$W_{oss} = \langle G\rangle - 1.9(\langle G_{\rm BP}\rangle - \langle G_{\rm BR}\rangle),$$

we are able to derive the stellar mass for each individual F- and FO-mode pulsator. The inferred stellar masses with the associated errors,[6] for the F- and FO-mode models, are reported in columns 9 and 10 of Table 2.

The top panel of Figure 2 shows the derived mass distribution histograms for the selected F (green bars) and FO (red bars) Gaia DR2 GCCs.

We notice that the selected GCC sample is predicted to cover a relatively wide range of masses, peaked around $5.6M_{\odot}$ and $5.4M_{\odot}$ for the F- and FO-mode pulsators, respectively. Interestingly enough, if the error on the measured parallaxes

[4] The Gaia filter Wesenheit function is defined as

$$W = \langle G\rangle - 1.9(\langle G_{\rm BP}\rangle - \langle G_{\rm BR}\rangle)$$

following the prescriptions by Ripepi et al. (2019).

[5] $\alpha = l/H_P$, where l is the length of the path covered by the convective elements and H_P is the local pressure height scale.

[6] The estimated errors take into account the uncertainty on the individual Gaia parallaxes, the intrinsic dispersion of the predicted PWM relations, and the error on the estimated W_{oss} considering a mean photometric error on the Gaia mean magnitudes of the order of 0.02 mag.

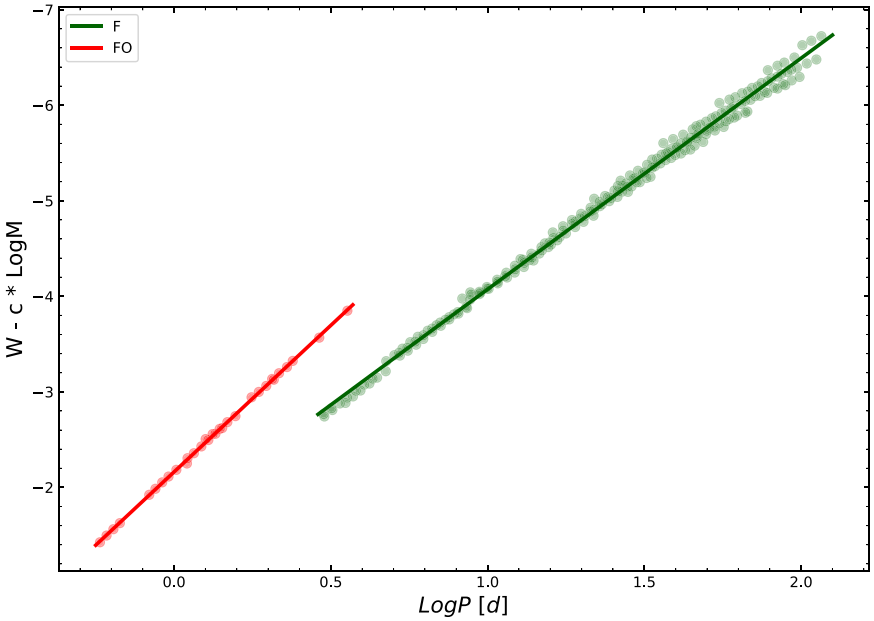

Figure 1. Projection of the inferred PWM relations and F (green symbols) and FO (red symbols) model distribution in the $W - c \log M$ vs.$\log P$ plane.

decreased, as expected in the next Gaia Data Releases, we would obtain a corresponding improvement in the precision of our mass determinations. In particular, a precision on parallaxes of the order of 1% would imply an error on the inferred stellar mass of the order of 2% and 3% in the case of the F and FO pulsators, respectively.

3.3. The Effect of the Gaia Parallax Offset

To take into account the Gaia DR2 Cepheid parallax offset corresponding to $\langle \Delta\varpi \rangle = 0.046 \pm 0.013$ mas and derived by Riess et al. (2018) through the comparison with Hubble Space Telescope space scan astrometric determinations (see Riess et al. 2018 for details), we performed again our mass derivation procedure for the F and FO GCCs by increasing the parallax values reported in Table 2 by $\langle \Delta\varpi \rangle = 0.046$ mas. The new estimated masses and the relative errors for the F- and FO-mode pulsators are reported in the last two columns of Table 2. The obtained results are shown in the bottom panel of Figure 2. We notice that the parallax offset effect moves the peak of the distribution to lower masses, around 5.2 $M_{\odot}$ and 5.1 $M_{\odot}$, for the F and FO modes, respectively. This occurrence is expected on the basis of the coefficients of the PWM relations. Indeed, an increase of the parallax implies a decrease in the distance modulus and, in turn, a fainter Wesenheit function, that at a fixed period, implies a lower mass. For the same reason, if the applied offset were $\langle \Delta\varpi \rangle = 0.046 + 0.013 = 0.059$ mas, the inferred masses would be on average smaller than the literature ones, while if an offset $\langle \Delta\varpi \rangle = 0.046 - 0.013 = 0.033$ mas were assumed, the inferred masses would become more discrepant with the literature ones with respect to Figure 3.

3.4. Comparison with the Literature

In the top panel of Figure 3 we show the behavior of the theoretical masses derived with the PWM relations including the DR2 parallax offset, as a function of the pulsation period, for the F (filled circles) and FO (open circles) mode GCCs, compared with the position of the Cepheids in binary systems for which independent mass estimates are available in Kervella et al. (2019, red symbols) and Evans et al. (2011, and references therein, cyan symbols). The general trend predicted by our theoretical scenario is in good agreement with the plotted data and the more recent determination of V350 Sgr mass (5.2 ± 0.3 $M_{\odot}$) by Evans et al. (2018). To better quantify this agreement, in the bottom panel we show the difference between our results and the ones by Kervella et al. (2019, red symbols) and Evans et al. (2011, cyan symbols) for the Cepheids in common with the two data sets. This plot confirms that we find a good agreement for most of the stars with the exception of RX Cam and U Vul for the F-mode. We notice that these two stars also deviate from more than 1σ from the empirical PW relation derived by Ripepi et al. (2019). For the FO V1334 Cyg our estimate with the assumed offset and the result by Kervella et al. (2019) are quite different but still consistent within the errors. The same occurs when the more recent determination of V1334 Cyg (4.288 ± 0.133 $M_{\odot}$) by Gallenne et al. (2018) is taken into account. We also verified that a worse agreement with literature mass values is obtained when no offset is applied to Gaia parallaxes.

4. Discussion

The results shown in the previous section suggest that a general good agreement can be found between our mass determinations based on Gaia DR2 parallaxes combined with new derived theoretical PWM relations and independent mass values obtained for Cepheids in binary systems in the literature. This occurrence supports the accuracy of current theoretical scenario and at the same time paves the way to future applications. In particular, we plan to apply the same theoretical tool to the next more accurate Gaia Data Releases in order to reduce the error on mass determinations at the level of few percent with relevant implications for our knowledge of both the present mass function and the ML relation of intermediate-mass He-burning stars in the Milky Way. Moreover, by extending the PWM relation to other bands (including LSST Vera Rubin filters) and chemical compositions, we will be able to (i) infer the mass distributions of Cepheid samples in

Table 2
The Individual Masses Estimated from the Theoretical PWM Relations Combined with Gaia DR2 Parallaxes, for the F- and FO-mode GCCs in the Selected Sample

Gaia DR2 Source Id	Mode	P(days)	G(mag)	$G_{\rm BP}$(mag)	G_{RP}(mag)	ϖ(mas)	$\sigma\varpi$(mas)	$M/M_{\odot}$	$\sigma M/M_{\odot}$	$M/M_{\odot}$ corr	$\sigma M/M_{\odot}$ corr
(1)	(2)	(3)	(4)	(5)	(6)	(7)	(8)	(9)	(10)	(11)	
1857884212378132096	F	4.43546	5.46	5.77	5.07	1.674	0.089	4.2	0.5	4.0	0.5
4066429066901946368	F	5.05787	6.82	7.37	6.23	1.119	0.053	5.2	0.6	4.8	0.5
5235910694044165760	F	3.08613	8.70	9.22	8.06	0.681	0.032	4.1	0.5	3.6	0.4
...	...	...	...	...	...	...	...	...	...		
5351436724362450304	FO	1.11936	11.09	11.62	10.41	0.389	0.030	3.3	0.7	2.4	0.5
2164475809937299584	FO	1.76585	10.18	10.74	9.49	0.343	0.027	7.6	1.7	5.4	1.2
5245796334347122944	FO	2.06344	8.09	8.53	7.54	0.858	0.026	3.5	0.4	3.0	0.3
...	...	...	...	...	...	...	...	...	...		

(This table is available in its entirety in machine-readable form.)

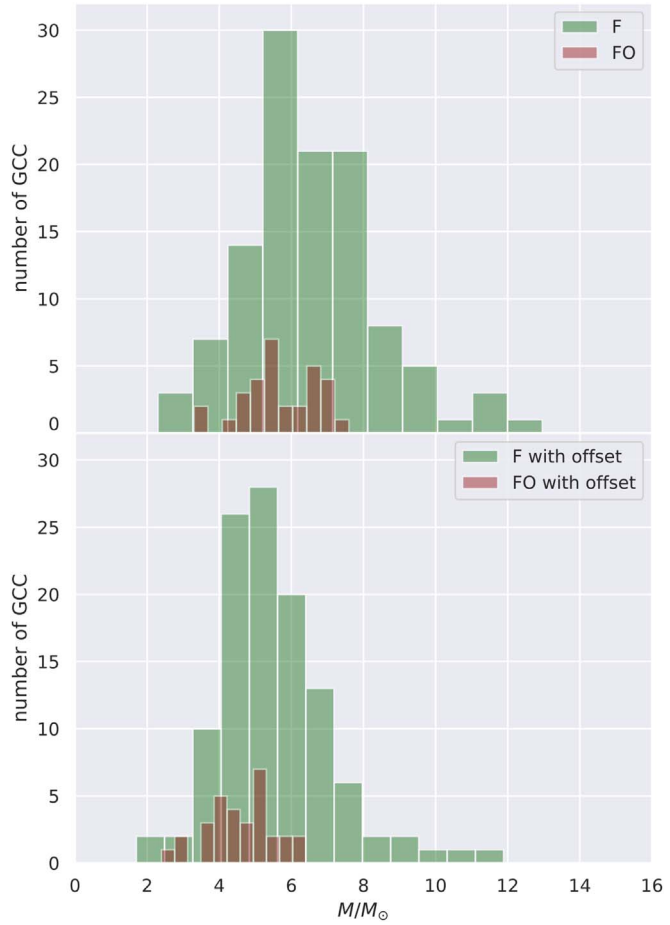

Figure 2. Top panel: the predicted mass distribution of the F (green bars) and FO (red bars) mode pulsators. Bottom panel: the same distribution as in the top panel, but obtained including the Gaia DR2 Cepheid parallax offset.

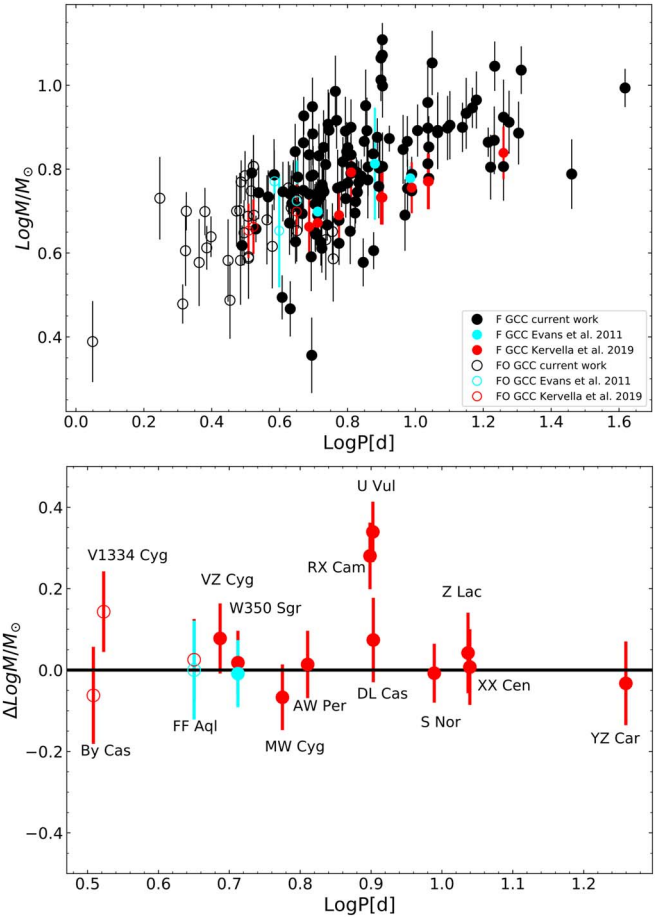

Figure 3. Top panel: the predicted mass distribution of the F (filled circles) and FO (open circles) pulsators as a function of the pulsation period. Bottom panel: the difference between our results and the ones by Kervella et al. (2019, red symbols) and Evans et al. (2011, cyan symbols) for the Cepheids in common with the two data sets.

the Local Group for which accurate distances, e.g., LSST astrometric distances, will become available; (ii) to constrain the coefficients of chemical abundances in theoretical Cepheid ML relations; and (iii) to predict the implications for the dependence of Cepheid properties and distance scale on the chemical composition. We notice that the PWM relation is expected to depend on metallicity because as the metallicity decreases, the theoretical quantity Mag-1.9*color is expected to get slightly fainter than in the solar case, according to previous results (see, e.g., Figure 9 in Caputo et al. 2000). Moreover, preliminary tests in the optical bands, based on the quoted previously computed models, suggest that the mass dependence of the PWM relation is reduced in lower-metallicity model sets, with the effect of predicting systematically higher masses at a fixed distance and period. On the other hand, by forcing the coincidence, within the errors, of our "uncorrected" mass evaluations as reported in columns 9 and 10 of Table 2, with the literature determinations by Kervella et al. and Evans et al. reported in Figure 3, we can derive an independent estimate of the offset that should be applied to Gaia DR2 parallaxes. In particular, by excluding RX Cam, U Vul, and DL Cas, as well as V1334 Cyg, which deviate by more than 1σ from the PW relations by Ripepi et al. (2019), we obtain a mean offset $\langle \Delta\varpi \rangle = 0.053 \pm 0.029$ mas, where the uncertainty is the standard error of the mean. This result is slightly higher than, but consistent within the errors, with the value obtained by Riess et al. (2018).

We thank the referee for pertinent and useful comments that significantly improved the content of this Letter. We acknowledge Istituto Nazionale di Fisica Nucleare (INFN), Naples section, specific initiative QGSKY. This work has made use of data from the European Space Agency (ESA) mission Gaia (https://www.cosmos.esa.int/gaia), processed by the Gaia Data Processing and Analysis Consortium (DPAC, https://www.cosmos.esa.int/web/gaia/dpac/consortium). Funding for the DPAC has been provided by national institutions, in particular the institutions participating in the Gaia Multilateral Agreement. In particular, the Italian participation in DPAC has been supported by Istituto Nazionale di Astrofisica (INAF) and the Agenzia Spaziale Italiana (ASI) through grants I/037/08/0, I/058/10/0, 2014-025-R.0, 2014-025-R.1.2015, and 2018-24-HH.0 to INAF (PI: M.G. Lattanzi). We acknowledge partial financial support from "Progetto Premiale" MIUR MITIC (PI: B. Garilli) and the INAF Main Stream SSH program, 1.05.01.86.28. This work has made use of the VizieR database, operated at CDS, Strasbourg, France.

ORCID iDs

Marcella Marconi https://orcid.org/0000-0002-1330-2927
Giulia De Somma https://orcid.org/0000-0002-5819-3461

Vincenzo Ripepi https://orcid.org/0000-0003-1801-426X
Roberto Molinaro https://orcid.org/0000-0003-3055-6002
Ilaria Musella https://orcid.org/0000-0001-5909-6615

References

Anderson, R. I., Saio, H., Ekström, S., Georgy, C., & Meynet, G. 2016, A&A, 591, A8
Bailey, J. E., Nagayama, T., Loisel, G. P., et al. 2015, Natur, 517, 56
Bhardwaj, A., Kanbur, S. M., Marconi, M., et al. 2017, EPJWC, 152, 01010
Bono, G., Caputo, F., Cassisi, S., et al. 2000, ApJ, 543, 955
Bono, G., Caputo, F., Castellani, V., & Marconi, M. 1999a, ApJ, 512, 711
Bono, G., Gieren, W. P., Marconi, M., Fouqué, P., & Caputo, F. 2001, ApJ, 563, 319
Bono, G., Marconi, M., & Stellingwerf, R. F. 1999b, ApJS, 122, 167
Bono, G., & Stellingwerf, R. F. 1994, ApJS, 93, 233
Caputo, F., Bono, G., Fiorentino, G., Marconi, M., & Musella, I. 2005, ApJ, 629, 1021
Caputo, F., Marconi, M., Musella, I., & Santolamazza, P. 2000, A&A, 359, 1059
Cassisi, S., & Salaris, M. 2011, ApJL, 728, L43
Chiosi, C., Wood, P. R., & Capitanio, N. 1993, ApJS, 86, 541
Clementini, G., Ripepi, V., Molinaro, R., et al. 2019, A&A, 622, A60
De Somma, G., Marconi, M., Molinaro, R., et al. 2020, ApJS, 247, 30
Evans, N. R., Berdnikov, L., Gorynya, N., Rastorguev, A., & Eaton, J. 2011, AJ, 142, 87
Evans, N. R., Proffitt, C., Carpenter, K. G., et al. 2018, ApJ, 866, 30
Freedman, W. L., Madore, B. F., Gibson, B. K., et al. 2001, ApJ, 553, 47
Gaia Collaboration, Brown, A. G. A., Vallenari, A., et al. 2018, A&A, 616, A1
Gaia Collaboration, Prusti, T., de Bruijne, J. H. J., et al. 2016, A&A, 595, A1
Gallenne, A., Kervella, P., Evans, N. R., et al. 2018, ApJ, 867, 121
Keller, S. C., & Wood, P. R. 2006, ApJ, 642, 834
Kervella, P., Gallenne, A., Evans, N. R., et al. 2019, A&A, 623, A117
Marconi, M., Molinaro, R., Bono, G., et al. 2013a, ApJL, 768, L6
Marconi, M., Molinaro, R., Ripepi, V., et al. 2017, MNRAS, 466, 3206
Marconi, M., Molinaro, R., Ripepi, V., Musella, I., & Brocato, E. 2013b, MNRAS, 428, 2185
Marconi, M., Musella, I., & Fiorentino, G. 2005, ApJ, 632, 590
Neilson, H. R., & Langer, N. 2012, A&A, 537, A26
Pietrzyński, G., Thompson, I. B., Gieren, W., et al. 2010, Natur, 468, 542
Pietrzyński, G., Thompson, I. B., Graczyk, D., et al. 2011, ApJL, 742, L20
Prada Moroni, P. G., Gennaro, M., Bono, G., et al. 2012, ApJ, 749, 108
Ragosta, F., Marconi, M., Molinaro, R., et al. 2019, MNRAS, 490, 4975
Riess, A. G., Casertano, S., Yuan, W., et al. 2018, ApJ, 861, 126
Riess, A. G., Casertano, S., Yuan, W., Macri, L. M., & Scolnic, D. 2019, ApJ, 876, 85
Riess, A. G., Macri, L., Casertano, S., et al. 2011, ApJ, 730, 119
Ripepi, V., Molinaro, R., Musella, I., et al. 2019, A&A, 625, A14